# Cell-penetrating peptide inhibits retromer-mediated human papillomavirus trafficking during virus entry

Pengwei Zhang[a], Ruben Moreno[b], Paul F. Lambert[b], and Daniel DiMaio[a,c,d,e,1]

[a]Department of Genetics, Yale School of Medicine, New Haven, CT 06520-8005; [b]McArdle Laboratory for Cancer Research, University of Wisconsin School of Medicine, Madison, WI 53705-2275; [c]Department of Therapeutic Radiology, Yale School of Medicine, New Haven, CT 06520-8040; [d]Department of Molecular Biophysics & Biochemistry, Yale School of Medicine, New Haven, CT 06520-8024; and [e]Yale Cancer Center, New Haven, CT 06520-8028

Edited by Thomas Shenk, Princeton University, Princeton, NJ, and approved February 3, 2020 (received for review October 16, 2019)

**Virus replication requires critical interactions between viral proteins and cellular proteins that mediate many aspects of infection, including the transport of viral genomes to the site of replication. In human papillomavirus (HPV) infection, the cellular protein complex known as retromer binds to the L2 capsid protein and sorts incoming virions into the retrograde transport pathway for trafficking to the nucleus. Here, we show that short synthetic peptides containing the HPV16 L2 retromer-binding site and a cell-penetrating sequence enter cells, sequester retromer from the incoming HPV pseudovirus, and inhibit HPV exit from the endosome, resulting in loss of viral components from cells and in a profound, dose-dependent block to infection. The peptide also inhibits cervicovaginal HPV16 pseudovirus infection in a mouse model. These results confirm the retromer-mediated model of retrograde HPV entry and validate intracellular virus trafficking as an antiviral target. More generally, inhibiting virus replication with agents that can enter cells and disrupt essential protein-protein interactions may be applicable in broad outline to many viruses.**

HPV | retromer | protein transduction domain | retrograde | antiviral agent

Human papillomaviruses (HPVs) are responsible for 5% of human cancer, including virtually all cervical cancer and most oropharyngeal cancer. Although highly efficacious HPV vaccines exist, they protect against only a subset of HPV types and do not clear existing infections, and there are no drugs that specifically inhibit HPV infection or spread. Mechanistic understanding of the HPV life cycle may lead to the development of rational molecular strategies for preventing or treating HPV infection. Such strategies could reduce the global burden of HPV-induced disease, particularly diseases caused by nonvaccine HPV types or occurring in people who are not vaccinated or who do not mount an effective immune response to vaccination.

HPVs are nonenveloped DNA viruses that contain 360 molecules of the L1 major capsid protein and up to 72 molecules of the L2 capsid protein. The L2 protein is required for proper trafficking of the incoming virus to the nucleus, the site of viral gene expression and DNA replication (1, 2). After HPV is internalized, a short sequence of basic amino acids near the C terminus of the L2 protein serves as a cell-penetrating peptide (CPP) to transfer a segment of the protein through the endosomal membrane into the cytoplasm (3). An L2 sequence [the retromer-binding site (RBS)] adjacent to the CPP then binds directly to retromer, a cytoplasmic cellular protein complex that sorts cellular proteins and the incoming virus particle into the retrograde transport pathway for trafficking to the trans-Golgi network (TGN) en route to the nucleus (4–8). Knock-down of retromer expression or mutations in the L2 protein that inhibit protrusion of the L2 protein into the cytoplasm or directly block retromer binding impair exit of HPV from the endosome and prevent trafficking of the virus to the TGN, thereby inhibiting infection (3, 6, 7).

Here, we developed peptides that disrupt retromer-mediated sorting of HPV into the retrograde transport pathway during infection. Short peptides containing the RBS from HPV16 L2 bind retromer in vitro and are able to transit across the plasma membrane (3, 7). Therefore, we hypothesized that the membrane-penetrating and retromer-binding activities of an L2 segment that normally mediates virus entry could be harnessed to inhibit infection. We show that peptides containing the L2 CPP and the adjacent RBS enter cells from the culture medium and bind retromer, thereby sequestering it from incoming HPV. This prevents endosome exit and trafficking of the incoming virus to the TGN, thereby aborting infection. These experiments formally establish the modular membrane-penetrating and retromer-binding activities of specific elements in the C terminus of L2 in infected cells, demonstrate that the retromer-HPV interaction can be disrupted in intact cells, and confirm the importance of retromer-mediated sorting of HPV into the retrograde pathway for successful infection. Importantly, our results also provide proof-of-principle that intracellular virus trafficking is a therapeutic vulnerability of HPV infection, and identify retromer binding as a potential antiviral target. More generally, inhibiting virus infection with cell-penetrating peptides and other agents that disrupt intracellular protein-protein interactions required for virus replication may be broadly applicable as an antiviral strategy.

## Results

We synthesized a 29-residue peptide, designated P16/16, that contains the RBS and the CPP from HPV16 L2 in the context of natural L2 sequences (Fig. 1*A*). This peptide is competent for

### Significance

**Human papillomaviruses (HPVs) are responsible for 5% of cancers, but no specific antiviral agents inhibit HPV infection. Based on our mechanistic understanding of HPV entry into cells, we designed a strategy to inhibit HPV infection. We demonstrate that short synthetic peptides derived from an HPV capsid protein enter cells, interfere with a protein interaction essential for intracellular virus trafficking, and prevent HPV from entering its proper intracellular transport pathway, thereby inhibiting infection in cultured cells and in mice. Thus, we have repurposed viral protein segments that normally mediate infection into a rationally designed agent that inhibits infection. The use of cell-penetrating peptides to disrupt essential intracellular protein-protein interactions may be broadly applicable in virology and in other situations.**

Author contributions: P.Z., R.M., P.F.L., and D.D. designed research; P.Z. and R.M. performed research; P.Z., R.M., P.F.L., and D.D. analyzed data; and P.Z. and D.D. wrote the paper.

Competing interest statement: P.Z. and D.D. are inventors on a patent application related to this work.

This article is a PNAS Direct Submission.



[1]To whom correspondence may be addressed. Email: daniel.dimaio@yale.edu.

This article contains supporting information online at https://www.pnas.org/lookup/suppl/doi:10.1073/pnas.1917748117/-/DCSupplemental.

First published March 2, 2020.

retromer binding in vitro (7). HeLa cells were preincubated for 1 h in medium containing various concentrations of P16/16 and then infected at a multiplicity of infection (MOI) of 1 with HPV16 pseudovirus (PsV), which consists of a complete L1 and L2 capsid containing a reporter plasmid that expresses the fluorescent protein HcRed (9). As shown in Fig. 1*B*, the L2 peptide caused a dose-dependent reduction in infection, as assessed by flow cytometry for HcRed fluorescence at 48 h postinfection (h.p.i.). Because this assay scores only early events in HPV infection, this result suggests that the peptide inhibited delivery of HPV PsV to the nucleus. Under these conditions, P16/16 displayed a half-maximal inhibitory concentration ($IC_{50}$) of 3.6 μM. Similar results were obtained with several independent batches of peptide. The peptide significantly inhibited PsV infection even at an MOI of 10 or 100, although inhibition was less pronounced at a high MOI (Fig. 1*C*). P16/16 also inhibited infection by authentic HPV16 produced in organotypic raft cultures, as assessed by quantitative reverse-transcriptase PCR for HPV E7 mRNA (Fig. 1*D*).

P16/16 also potently inhibited infection by HPV18 and HPV5 PsVs (Fig. 2), which are other HPV types known to be dependent on retromer (10). HPV18 is a high-risk oncogenic HPV type that, like HPV16, infects genital mucosa, and HPV5 is a divergent HPV type associated with skin warts and cancer. In addition, P16/16 inhibited infection by HPV16 PsV in HaCaT skin keratinocytes as well as in HeLa cells (Fig. 1*E*). In contrast, P16/16 did not inhibit infection by SV40 (*SI Appendix*, Fig. S1*A*), an unrelated nonenveloped small DNA tumor virus that does not require retromer for infection (6). We observed no apparent toxicity of the peptides based on cell morphology and cell viability assay for up to 72 h of treatment at an effective antiviral dose of the peptide (*SI Appendix*, Fig. S1*B*).

Inhibition of HPV16 PsV infection by P16/16 treatment persisted for at least 96 h.p.i. (*SI Appendix*, Fig. S1*C*, orange curves). Furthermore, if P16/16 and HPV were removed from the medium at 24 h.p.i., infection was not restored over the next three days (Fig. 1*C*, green curves), suggesting that the peptide caused sustained and possibly irreversible inhibition of infection. We also tested if removal of the peptide from the medium prior to infection abrogated the inhibitory effect. We pretreated cells with peptide for 24 h, removed peptide from the culture medium, and then infected cells at various times after peptide removal. As shown in Fig. 1*F*, significant inhibition still occurred if HPV PsV was added 48 h after peptide removal, but it was less pronounced than when the virus was added soon after peptide removal.

To identify elements in the peptide required for inhibition of HPV infection, we tested the activity of mutant peptides (Fig. 1*A*). As shown in Fig. 2, the inhibitory effect was eliminated by mutations in the CPP (peptides designated P16/6A and P16/3R) or the RBS [double mutant (DM) peptide designated PDM/16]. These CPP and RBS mutations block membrane protrusion and retromer binding, respectively (3, 7). Thus, both cell-penetrating and retromer-binding activity were required for HPV inhibition. In addition, the HPV16 CPP in P16/16 could be

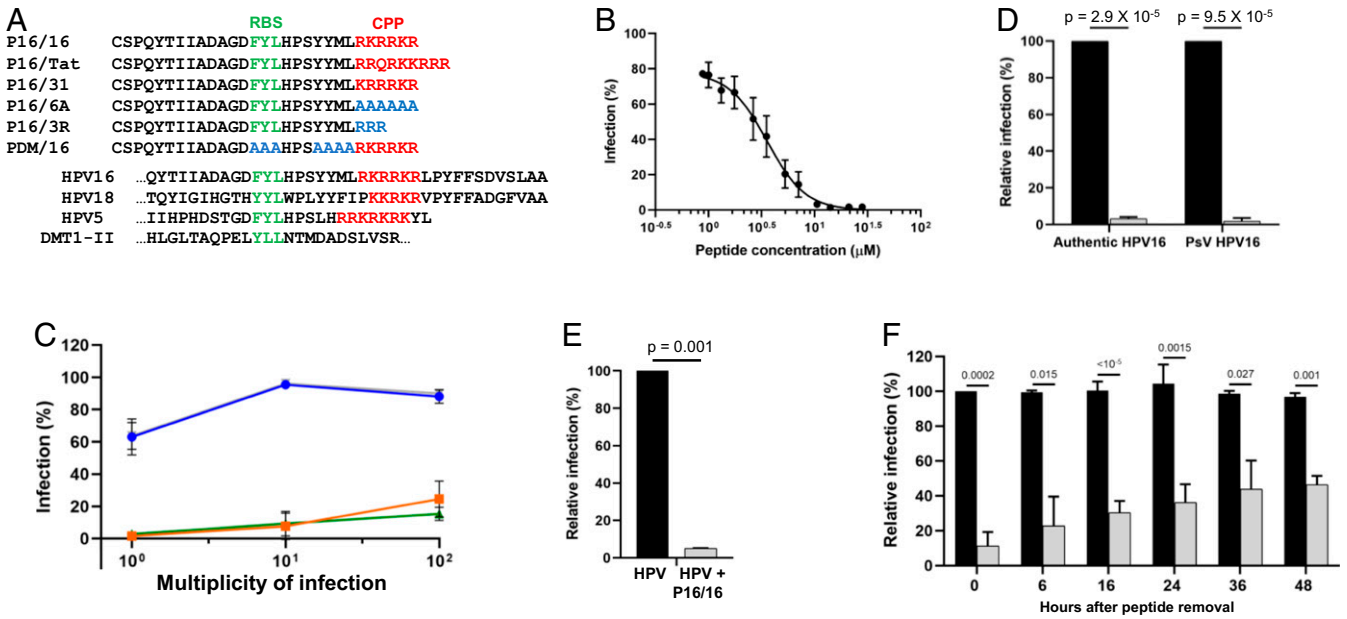


**Fig. 1.** Identification and analysis of peptides that inhibit HPV infection. (*A*, *Top*) Sequences of L2 peptides with wild-type CPP segments (red) and RBS (green) highlighted. Amino acid substitutions in the CPP or RBS mutant peptides are shown in blue. (*A*, *Bottom*) RBS and flanking sequences of indicated HPV L2 proteins or DMT1-II. (*B*) Inhibitory dose–response curve for the wild-type P16/16 peptide. HeLa cells were pretreated with various concentrations of P16/16 for 1 h prior to infection with HPV16 PsV at an MOI of 1. The peptide and PsV were left in the medium for the duration of the experiment. At 48 h.p.i., flow cytometry was used to determine the fraction of cells expressing reporter protein HcRed. The graph shows mean results of three experiments, +/− SD. (*C*) HeLa cells were pretreated for 1 h with 14 μM (orange line) or 28 μM (green line) P16/16 or 14 μM PDM/16 (gray line), or left untreated (blue line). Cells were then infected with HPV16 PsV at the indicated MOI, and at 48 h.p.i. infectivity was measured by flow cytometry for reporter gene expression as in *B*. (*D*) Inhibition of authentic HPV16. HeLa cells were infected with HPV16 harvested from organotypic cultures of human keratinocytes or with HPV16 PsV in the presence (gray bars) or absence (black bars) of 14 μM P16/16. Infection by HPV16 and HPV16 PsV was assessed by qRT-PCR for expression of HPV E7 and HcRed mRNA, respectively, and normalized to infection by the cognate virus in the absence of the peptide. The graph shows average results of three independent experiments, +/− SD, where infection of untreated cells is set at 100%. The background signal determined with noncognate primers was <0.01%. (*E*) Inhibition of HPV infection of HaCaT cells. HaCaT keratinocytes were infected at an MOI of 1 with HPV16 PsV in the presence (gray bars) or absence (black bars) of 14 μM P16/16, and infectivity was assessed at 48 h.p.i. by flow cytometry for HcRed fluorescence and displayed as in *B*. (*F*) HeLa cells were treated for 24 h with no peptide (black bars) or 14 μM P16/16 (gray bars). The peptide was then removed, and the cells were incubated for the indicated period of time prior to infection with HPV16 PsV at an MOI of 1. At 48 h.p.i, infectivity was measured by flow cytometry as in Fig. 1*B*. The graph shows results of three experiments +/− SD, normalized to no peptide control at time = 0. Numbers indicate the *P* value for each pairwise comparison.

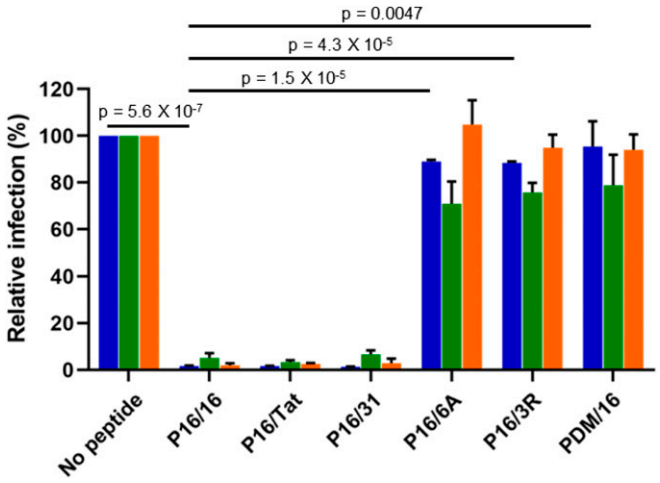


**Fig. 2.** Identification of sequence elements required for inhibition of multiple HPV types. HeLa cells were pretreated with 14 μM indicated peptide for 1 h, followed by infection with HPV16 (blue), HPV18 (green), or HPV5 PsV (orange) at an MOI of 1. Peptides and PsV were left in the medium for the duration of the experiment. As a control, cells were incubated with the solution used to dissolve the peptide. At 48 h.p.i., flow cytometry was used to determine the fraction of cells expressing HcRed. The graph shows average results of three independent experiments, +/− SD, normalized to infection of each PsV type in the absence of the peptide. P16/16, P16/Tat, and P16/31 caused statistically significant ($P < 0.01$ or lower) inhibition of all three PsV types, which was blocked by the mutations. *P* values are shown for comparison of P16/16 and no peptide, P16/6A, P16/3R, and PDM/16 for HPV16 PsV. Similar levels of significance were achieved with these peptides and HPV18 and HPV5 PsV.

replaced by the CPP from HIV Tat [designated P16/Tat (11)] or HPV31 [designated P16/31 (3)] without loss of activity against the three HPV PsV types tested (Figs. 1*A* and 2). These results show that the prototypic CPP from Tat and a CPP from a second HPV type also deliver a biologically active RBS into cells.

We used biotinylated P16/16 and PDM/16 (bP16/16 and bPDM/16, respectively) to confirm their entry into cells, determine their intracellular location and persistence, and test if they bind retromer in intact cells. We previously showed that wild-type bP16/16 but not the mutant bPDM/16 peptide pulled down retromer from cell extracts (7). Biotinylation did not affect the anti-HPV activity of P16/16 (*SI Appendix*, Fig. S1*D*). To test peptide uptake, uninfected HeLa cells were incubated with bP16/16 or bPDM/16 for three hours. Cells were then washed to remove unbound peptide, permeabilized, and stained with fluorescent streptavidin, which binds tightly to biotin, and with an antibody that recognizes the retromer subunit vacuolar protein sorting-associated protein 35 (VPS35). Confocal microscopy showed that bP16/16 was localized to large cytoplasmic puncta superimposed on a more diffuse cytoplasmic distribution (Fig. 3*A*, *Middle*). Strikingly, the mutant bPDM/16 showed only the diffuse distribution (Fig. 3*A*, *Bottom*). These results show that peptides rapidly enter cells and suggest that retromer binding is required for the punctate signal. VPS35 also displayed a punctate distribution in the presence or absence of peptides. Importantly, there was significant colocalization of VPS35 with bP16/16 but not with bPDM/16, showing that the wild-type but not the mutant peptide stably associated with retromer in intact cells (Fig. 3 *A* and *B*). Detectable intracellular peptide persisted for at least 48 h after removal of peptide from the medium (Fig. 3*C*), consistent with the inhibitory effect of the peptide at this time point as reported above (Fig. 1*F*).

To test whether the L2 peptide inhibited the ability of retromer to bind incoming HPV16 PsV, we conducted a proximity ligation assay (PLA), which generates a fluorescent signal when two antigens are within 40 nm of each other (10, 12). Fig. 3*D* shows that at 8 h.p.i., the PLA for HPV16 L1 and VPS35 detected interaction of the incoming virus with retromer in intact HeLa cells, as previously reported (7). Strikingly, the wild-type P16/16 peptide inhibited the interaction of retromer with HPV, whereas the mutant peptide lacking the RBS did not (Fig. 3 *D* and *E*). Together, these data show that the peptide containing the CPP and the RBS enters cells, associates with retromer, and inhibits binding of retromer to the incoming virus.

Retromer knockdown or L2 mutations that interfere with retromer binding inhibit the exit of HPV from the endosome and prevent trafficking of the virus to the TGN (3, 6, 7). To test whether the inhibitory peptide has a similar effect, we identified the step of infection blocked by P16/16. First, for effective inhibition, the peptide needed to be added during the first few hours of infection (*SI Appendix*, Fig. S2*A*), suggesting that it inhibited a relatively early step in HPV entry. Immunofluorescence studies with an anti-L1 antibody showed that P16/16 did not inhibit HPV internalization (*SI Appendix*, Fig. S2*B*). We then used PLA to examine the localization of incoming HPV16 PsV in HeLa cells. The PLA for L1 and the endosome marker early ensodome antigen 1 (EEA1) confirmed the presence of HPV at the endosome at 8 h.p.i., regardless of treatment with the peptide, confirming that the peptide did not block HPV internalization. By 16 h.p.i., in untreated cells the virus was largely absent from the endosome because it departed to the TGN, as previously reported (8) (Fig. 4*A*). In contrast, EEA1-L1 PLA at 16 h.p.i. showed striking accumulation of HPV in the endosome of cells treated with P16/16. Consistent with this finding, at 16 h.p.i the PLA for L1 and the TGN marker, TGN46, showed that P16/16 inhibited the arrival of HPV in the TGN (Fig. 4*B*). We also assessed the localization of viral DNA by staining for the encapsidated reporter plasmid labeled with the nucleoside analog EdU. There was no EdU staining in mock-infected cells. After infection, P16/16 treatment resulted in retention of viral genomes in the endosome at 16 h.p.i. and failure of the genome to reach the TGN at 24 or 48 h.p.i. (*SI Appendix*, Fig. S3 *A* and *B*). By 48 h.p.i., in the absence of the peptide there was abundant EdU staining, including clear nuclear staining overlapping with or adjacent to the nuclear promyelocytic leukemia protein (PML), as reported by Day et al. (13) (Fig. 4*C*). P16/16 reduced overall EdU staining at this time point and abolished nuclear EdU staining, demonstrating that peptide treatment prevented transport of encapsidated DNA to the nucleus. Taken together, these experiments showed that the active peptide inhibited the exit of HPV from the endosome and its appearance in downstream retrograde compartments and the nucleus.

We also performed experiments at various times after infection to examine the fate of HPV after peptide inhibition. As shown in Fig. 5*A*, HPV16 L1 and FLAG-tagged L2 showed punctate, cytoplasmic distribution without nuclear staining at 8 h.p.i. in cells whether or not they were treated with the peptide. By 16 h.p.i., L1 and L2 in untreated cells showed obvious nuclear staining. P16/16 caused a striking redistribution of L1 and L2 by 16 h.p.i., with a reduction in nuclear staining for both proteins. This is consistent with an arrest in entry because at least some L1 and L2 accompanied the viral DNA to the nucleus during successful infection (13–15). At 24 h.p.i., the nuclear exclusion of L1 in P16/16-treated cells persisted and, most notably, there was a complete absence of L2 staining (Fig. 5*A*). Immunoblotting at 16 and 24 h.p.i. also showed a reduction in L1 and FLAG-tagged L2 in peptide-treated cells (Fig. 5*B*). Furthermore, as shown earlier, there were reduced levels of nuclear and nonnuclear input viral genomes at 48 h.p.i. (Fig. 4*C*). Taken together, these results suggest that blocking endosome exit resulted in the degradation of viral capsid proteins and DNA. To determine if the peptide directed the HPV to the lysosome for degradation, we assessed colocalization of L2 and the lysosomal marker lysosomal-associated

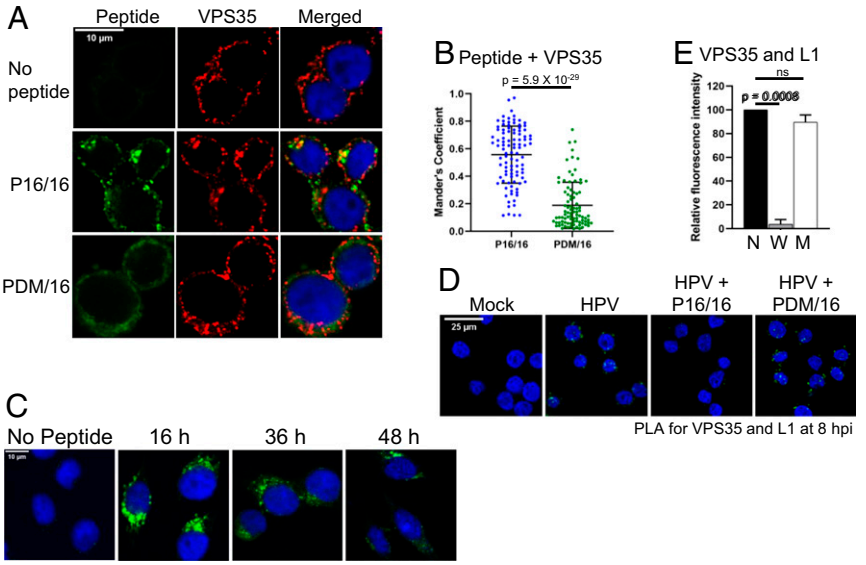


**Fig. 3.** The peptide binds retromer and blocks retromer association with HPV. (*A*) Uninfected HeLa cells were incubated with 14 μM bP16/16 or bPDM/16 for 3 h. Cells were then fixed, permeabilized, and stained with Alexa Fluor streptavidin (green) and an antibody recognizing the retromer subunit, VPS35 (red). The overlapping signal is pseudocolored yellow in the merged panels. Nuclei were stained blue with DAPI. Cells were imaged by confocal microscopy. (*B*) Mander's correlation coefficients for overlap between streptavidin and VPS35, with each spot representing the data for an individual cell. Approximately 100 cells were analyzed for each condition. Each dot represents data from a single cell. Horizontal lines show mean and SD. (*C*) HeLa cells were treated for 6 h with bP16/16. Medium was replaced with fresh medium without the peptide and the cells were incubated at 37 °C for the indicated period of time before staining with fluorescent streptavidin as in *A*. (*D*) HeLa cells were incubated for 1 h without the peptide or with 14 μM P16/16 or PDM/16, followed by mock-infection or infection with HPV16 PsV at an MOI of 200. At 8 h.p.i., cells were fixed and processed for PLA with anti-L1 and anti-VPS35 antibodies. The PLA signal is green, and the nuclei are stained blue with DAPI. Cells were imaged by confocal microscopy. (*E*) Approximately 200 cells in each sample were imaged. Images were processed by Fiji software and analyzed by BlobFinder software to measure total fluorescence intensity per cell in each sample. The graph shows the mean fluorescence per cell and SD, normalized to that of cells infected with wild-type HPV16 PsV in the absence of the peptide from three independent experiments (N, HPV no peptide; W, HPV + P16/16; M, HPV + PDM/16; n.s., not significant).

membrane protein 1 (LAMP1). As shown in Fig. 5 *C* and *D*, there was *less* colocalization in cells treated with P16/16. This lack of colocalization was more dramatic in the presence of the lysosomal inhibitor chloroquine (CQ), which caused a marked increase in L2 and LAMP1 colocalization in untreated cells but not in cells treated with P16/16 (Fig. 5 *C* and *D*). Similarly, as assessed by immunoblotting, CQ increased L1 and L2 levels in cells in the absence of P16/16 but did not reverse the reduced levels of viral proteins in cells treated with peptide (Fig. 5*E*).

Because retromer normally supports retrograde trafficking of cellular transmembrane proteins, we tested whether the L2 peptide inhibits transport of a cellular retromer cargo. We analyzed divalent metal transporter 1 isoform II (DMT1-II), a multipass transmembrane protein that is transported to the TGN in a retromer-dependent fashion (16, 17). We transfected HeLa cells with a plasmid expressing green fluorescent protein (GFP) fused to DMT1-II, and 6 h later cells were treated with P16/16 or PDM/16 or left untreated. The distribution of GFP fluorescence and anti-TGN46 antibody staining was assessed ~20 h later by confocal microscopy. As shown in *SI Appendix*, Fig. S4 *A* and *B*, GFP-DMT1-II and TGN46 in untreated cells showed a cytoplasmic distribution with a concentrated juxtanuclear pattern with considerable overlap (Mander's correlation coefficient, 0.33), as expected. In contrast, treatment with P16/16 caused GFP-DMT1-II to redistribute to a more diffuse localization with significantly less overlap with TGN46, whereas the mutant peptide PDM/16 had minimal effect on GFP-DMT1-II distribution (Mander's correlation coefficient, 0.17 vs. 0.28). Similarly, P16/16 but not PDM/16 caused the accumulation of GFP-DMT1-II in endosomes, as assessed by overlap of GFP fluorescence and EEA1 staining (*SI Appendix*, Fig. S4 *C* and *D*). Neither peptide affected the distribution of TGN46 or EEA1 staining. These results show that cytoplasmic delivery of a peptide containing the HPV16 RBS also inhibited trafficking of DMT1-II from the endosome to the TGN.

Finally, we tested if the L2 peptide inhibits HPV16 PsV infection in an established cervicovaginal challenge model in mice. Female Friend leukemia virus B (FVB) mice were treated with Depo-Provera and nonoxynol-9 to thin and chemically injure the cervicovaginal epithelium. Mice were then infected with HPV16 PsV expressing luciferase, as previously described (18). Some mice received PsV formulated in 25 μg P16/16 or PDM/16. At two days after infection, reproductive tissues were harvested and luciferase activity was measured. As shown in Fig. 6, in untreated samples HPV16 infection induced luciferase activity with considerable variability among individual mice, as previously described (18). P16/16 caused a reduction in luciferase expression with marginal statistical significance ($P = 0.088$ by the two-sided Wilcoxon rank sum test), while the mutant PDM/16 peptide lacking the RBS had no significant effect ($P = 0.38$). However, the more important comparison, which takes into account nonspecific effects of peptide treatment, is the difference between the wild-type peptide and the mutant peptide lacking the RBS, which shows that the wild-type peptide is significantly more inhibitory than the mutant ($P = 0.01$). These results show that the cell-penetrating peptide containing the L2 RBS inhibited HPV infection in an animal model. We also note that the peptides caused no overt toxicity in mice.

## Discussion

We showed that a CPP could deliver soluble peptides containing the HPV16 RBS into cultured cells, where it sequestered retromer from the virion and inhibited endosome exit of the virus, thereby aborting infection. The peptide with the wild-type RBS but not the mutant peptide also inhibited cervicovaginal HPV infection in female mice, implying that the peptide is not inactivated

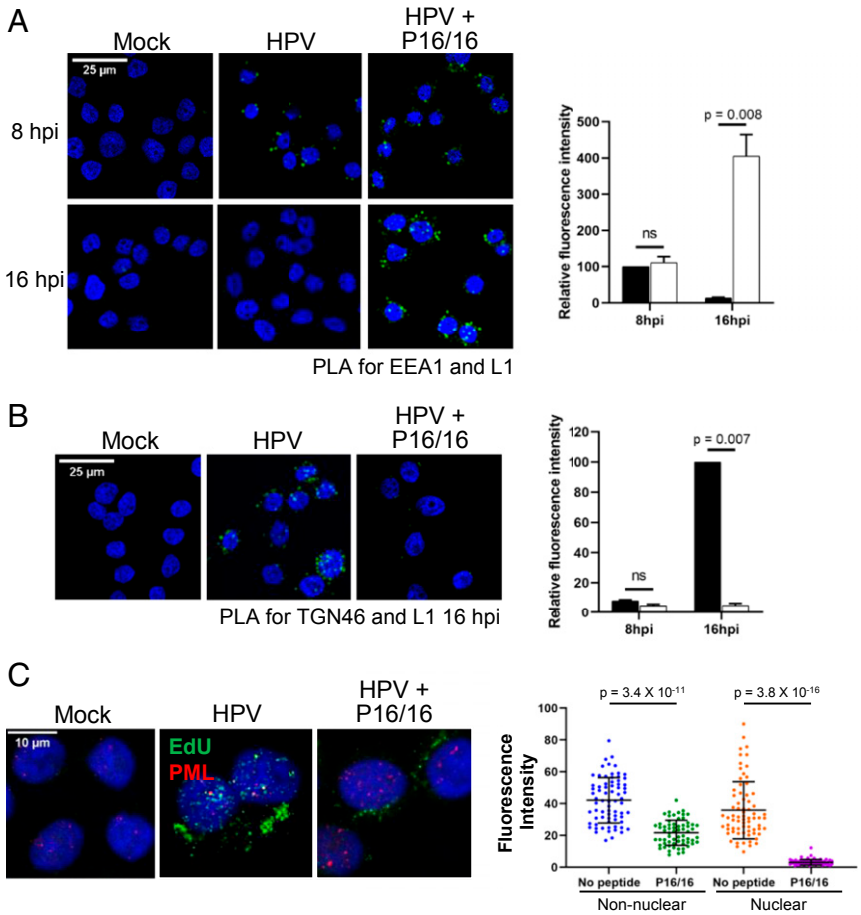


**Fig. 4.** The peptide inhibits HPV exit from the endosome. HeLa cells were incubated for 1 h with or without 14 μM P16/16, followed by mock-infection or infection with HPV16 PsV at an MOI of 200. At 8 and 16 h.p.i., PLA was performed as described in Fig. 3*D* with anti-L1 and anti-EEA1 antibody (*A*) or TGN46 antibody (*B*). The PLA signal for EEA1-L1 was normalized to that of cells infected with HPV16 PsV in the absence of peptide at 8 h.p.i., and the TGN46-L1 signal was normalized to untreated cells at 16 h.p.i. The graphs show average normalized fluorescence per cell and SD for three independent experiments (n.s., not significant). (*C*, *Left*) HeLa cells were mock-infected or infected with HPV16 PsV containing EdU-labeled reporter plasmid DNA at an MOI of 50. Where indicated, cells were pretreated for 1 h with 14 μM P16/16. At 48 h.p.i., cells were fixed and treated with Click-iT chemistry to stain viral DNA (green) and incubated with anti-PML antibody (red). The overlap in EdU and PML staining is pseudocolored yellow. Nuclei are stained blue. (*C*, *Right*) Nuclear and nonnuclear EdU staining as in *C, Left*, was quantified for 60 cells in each condition. Each dot represents data from an individual cell. Horizontal lines indicate mean and SD.

in the female reproductive tract and is able to access basal keratinocytes in this tissue, which support HPV infection. These results provide strong support for the retromer-mediated HPV entry model, independent of previous evidence based on analysis of viral mutants and retromer knock-down. This approach was made possible by use of a CPP to transfer the RBS across the plasma membrane into the cytoplasm and by the fact that a short linear sequence in L2 is sufficient for retromer binding. Notably, neither the cell-penetration nor retromer-binding activity required the rest of the L2 protein or the intact HPV capsid structure to enter and function in cells. Stable association with retromer, visualized by punctate RBS-dependent colocalization with VPS35, directly demonstrated that the peptide reached the cytoplasm. Delivery of peptides into cells in a biologically active form is often limited by their inefficient escape from the endosome into the cytoplasm (19), but the papillomavirus L2 CPPs have been optimized by hundreds of millions of years of evolution to penetrate the endosomal membrane and enter the cytoplasm to support infection. Therefore, papillomavirus CPPs and flanking sequences may be particularly effective as peptide delivery agents that can escape the endosome. The CPP from HIV Tat fused to C-terminal L2 sequences normally flanking the minimal HPV CPP also mediated entry of the inhibitory peptide in an active form.

Our results also provide insight about HPV trafficking. Most notably, interference with retromer binding causes accumulation of endosomal HPV at 16 h.p.i., but the virus does not persist in this compartment. Rather, by 24 h.p.i. L2 is no longer visible by immunofluorescence and by 48 h.p.i. total viral genome staining is reduced. These results show that the cells possess a mechanism to remove the incoming virus if it does not engage retromer, and they imply that transient inhibition of infection at this step imposes an irreversible block to infection. The persistent inhibition of infection even after removal of the peptide after 24 h (*SI Appendix*, Fig. S1*C*) is consistent with this interpretation. Elimination of viral components after peptide-induced inhibition does not appear to involve the lysosome.

The active peptide used here did not display toxicity at doses that inhibited HPV infection even though it affected trafficking of DMT1-II. In addition, we note that retromer knock-out cells are viable (e.g., refs. 20 and 21). Thus, HPV infection is more sensitive to retromer inhibition than is cellular viability, likely because HPV entry requires retrograde transport whereas cellular cargos are replenished by new synthesis as well as by retrograde

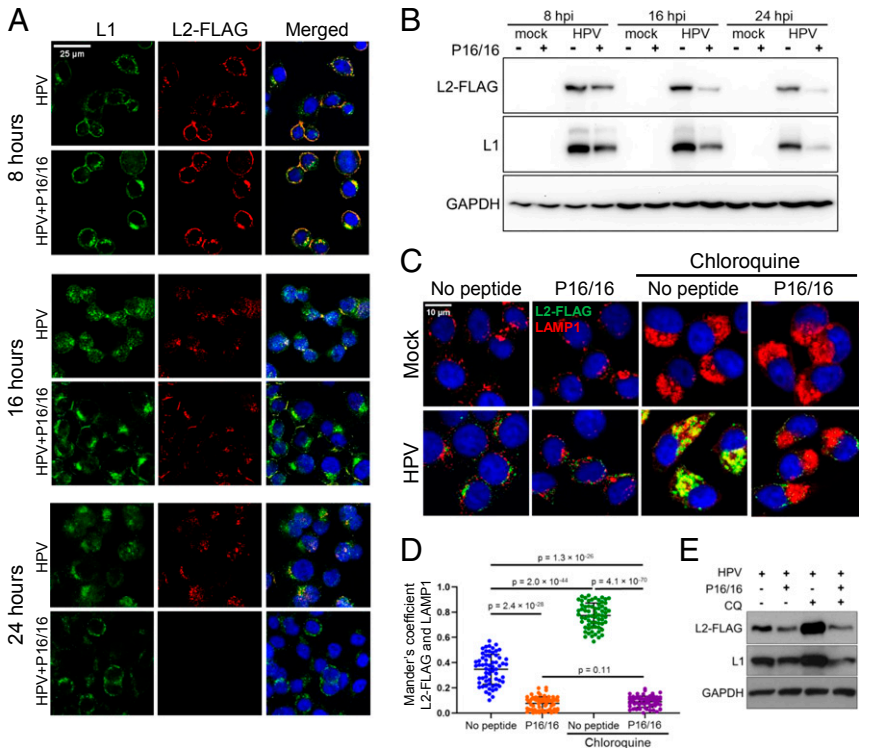


**Fig. 5.** Fate of HPV following peptide inhibition. (*A*) HeLa cells were incubated for 1 h with or without 14μM P16/16, followed by mock-infection or infection with HPV16 PsV containing FLAG-tagged L2 at an MOI of 50. At the indicated times after infection, cells were permeabilized and stained with anti-FLAG (red) and anti-L1 (green) antibody. Nuclei are stained blue. The overlap in FLAG and L1 staining is pseudocolored yellow in the merged panels. There was no antibody staining in mock-infected cells. (*B*) Cells pretreated with 14 μM P16/16 (+) or left untreated (–) were mock-infected or infected with HPV16 PsV at an MOI of 20 as in *A*. At the indicated h.p.i., extracts were prepared and assessed by immunoblotting for L1 and L2 expression. GADPH acts as a loading control. (*C*) Cells treated with P16/16 or left untreated were infected as in *A*. Where indicated, cells were treated with 100 μM chloroquine starting 30 min prior to infection. At 16 h.p.i., cells were permeabilized and stained with anti-FLAG (green) and anti-LAMP1 (red) antibodies. Nuclei are stained blue. The overlap between FLAG and LAMP1 staining is pseudocolored yellow. (*D*) Overlapping staining as in *C* was quantified as in Fig. 3*B*. (*E*) Cells were infected and treated with p16/16 and chloroquine (CQ) as in *C*. Extracts were prepared at 16 h.p.i and analyzed by immunoblotting.

transport. It may be possible to increase the potency of inhibitory peptides by multimerization of the CPP or the RBS, use of a CPP or RBS from other sources (including other HPV types), or other mutation or modification of the peptide sequence. However, manipulations that increase peptide potency may also increase toxicity.

Retromer has also been implicated in the life cycle of other viruses including hepatitis C virus, influenza virus, adeno-associated virus, HIV, and possibly poxviruses (22–28). Therefore, the peptides described here as well as other agents that target retromer may affect infection by these viruses as well. These peptides may also be useful probes of retromer function in noninfected cells.

While this work was being prepared for publication, Yan et al. (29) reported that short membrane-anchored lipopeptides derived from the N terminus of HPV L2 inhibited HPV infection with high potency. The peptides prevented arrival of HPV at the TGN, but the mechanism of inhibition was not explored. Although the N-terminal segment of L2 is required during normal HPV infection, its role in infection is not known. Nevertheless, the ability of peptides from either the N terminus or the C terminus of L2 to inhibit HPV infection suggests that the L2 protein and possibly other viral proteins may be a rich source of protein segments with antiviral activity.

Antiviral agents in clinical use act by relatively few mechanisms. Most inhibit viral enzymes, and a limited number of drugs inhibit cell surface binding, internalization, viral-cell membrane fusion, or virus uncoating (e.g., refs. 30–33). Our results validate intracellular virus trafficking as a therapeutic vulnerability. Because all known HPV L2 proteins appear to contain an RBS, agents that compete for retromer binding are likely to inhibit all HPV types. An entry inhibitor is not expected to cure an established HPV infection, although it would presumably inhibit the spread of HPV infection and possibly limit the persistence or recurrence of disease that is sustained by HPV reinfection in an individual. Because HPV is a localized infection of skin and mucous membranes requiring direct contact with an infected individual, a short-duration topical application of an HPV entry inhibitor might be useful in preventing genital HPV infection with minimal toxicity. In addition, most cutaneous HPV types are not included in current vaccines, so there are no other preventative options. More generally, our results provide proof-of-principle for an antiviral strategy—namely, the use of a cell-penetrating peptide to inhibit an essential interaction between a viral protein and the intracellular machinery required for virus replication. Although there are challenges to using peptides therapeutically, the identification of a required intracellular protein-protein interaction susceptible to disruption might inspire the development of more drug-like agents that block this interaction. Approaches based on this strategy may be applicable to many enveloped and nonenveloped viruses as well as in other settings to disrupt pathogenic intracellular protein-protein interactions that do not involve viral infection.

## Materials and Methods

**Cells, Plasmids, Virus, and Peptides.** HeLa-S3 cells (herein, HeLa cells) were obtained from the American Type Culture Collection. HaCaT keratinocytes were purchased from AddexBio Technologies. We obtained 293TT and 293FT cells from Christopher Buck (NIH) and Invitrogen, respectively. The plasmids p16sheLL, p18sheLL, and p5sheLL used for pseudovirus production and pCLucF

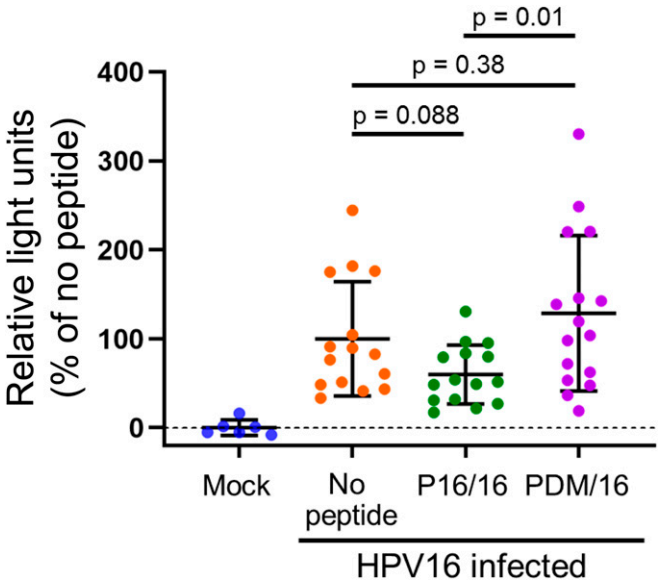


**Fig. 6.** The peptide inhibits HPV pseudovirus infection in vivo. Female FVB mice were treated with Depo-Provera and Conceptrol as described in *Materials and Methods*. Mice were then treated intravaginally with 4% carboxymethyl cellulose (CMC) (designated mock) or 4% CMC containing $3 \times 10^5$ transducing units of HPV16:pCLucF plus or minus 25 μg of P16/16 or PDM/16. Two days later, reproductive tract tissues were harvested and assayed in triplicate in vitro for luciferase activity, which is reported as relative light units per μg total protein. Each dot represents data from an individual mouse. Statistical analyses were made with the two-sided Wilcoxon Rank Sum test.

were gifts of Christopher Buck. pCAG-HcRed reporter plasmid was purchased from Addgene.

HPV PsV containing pGAG-HcRed or pCLucF was produced in 293TT or 293FT cells as described (9). HPV16 prepared in organotypic raft cultures was the generous gift of Craig Meyers (Hershey Medical Center). SV40 was prepared in CV1 cells as described (34). The infectious MOI of HPV PsV was determined by flow cytometry for reporter gene expression after infection of HeLa or 293FT cells with dilutions of PsV in the absence of the peptide.

Peptides were purchased from ABclonal Technology at >95% purity. Peptides were dissolved in 30% acetic acid and dimethyl-formamide and then diluted in sterile deionized water containing 0.01% sodium azide to a stock peptide concentration of 5 mg/mL.

**Infectivity.** To assess the effect of peptides on viral infection, HeLa and HaCaT cells were, in most cases, pretreated with peptides for 1 h, followed by infection with HPV PsV at 37 °C at an MOI of 1. The peptides and PsV were left in the medium for the duration of the experiment unless otherwise indicated. As a control, cells were incubated with the solution used to dissolve the peptides. Cells were assessed for HcRed fluorescence by flow cytometry to determine reporter protein expression at 48 h.p.i. In some experiments, cells were infected at various times after peptide removal or the peptide was added at various times after infection. To measure inhibition of authentic HPV16, HeLa cells were infected with raft-derived HPV16 or with HPV16 PsV at an MOI of 1 in the presence and absence of 14 μM P16/16. Total RNA was isolated 48 h.p.i., and HPV16 E7 RNA was measured by qRT-PCR. HcRed RNA from cells infected with HPV16 PsV was measured as a control.

For SV40, HeLa cells were incubated with 14 μM P16/16 or vehicle for 1 h and then infected with SV40 at an MOI of ∼1. At 48 h.p.i., samples were stained with antilarge T antigen antibody and assayed by flow cytometry.

**Internalization of Peptides.** To visualize the peptide in intact cells, HeLa cells were incubated for 3 or 6 h with 14 μM biotinylated bP16/16 or bPDM/16 peptides. Cells were then washed and immediately stained with Alexa Fluor 488 streptavidin conjugate and anti-VPS35 antibody or incubated in the absence of the peptide for various times before staining. Cells were imaged by confocal microscopy.

**Immunofluorescence Microscopy and Proximity Ligation Assay.** For PsV internalization experiments, HeLa cells were incubated for 1 h with or without 14 μM P16/16, and then mock-infected or infected with HPV16 PsV at an MOI of 50. After incubation at 4 °C for 2 h, cells were washed and shifted to 37 °C to initiate infection. At 8 or 16 h.p.i., samples were fixed, permeabilized, and stained with anti-L1 antibody. Cells were imaged by confocal microscopy.

For the proximity ligation assay, after 1-h incubation with peptides HeLa cells were infected with wild-type PsV at an MOI of 200. Infected cells were fixed and permeabilized at 8 or 16 h.p.i. and incubated with anti-L1 antibody and an antibody recognizing EEA1, TGN46, or VPS35. PLA was performed with Duolink reagents from Olink Biosciences according to the manufacturer's directions (10). Cells were imaged by confocal microscopy.

**Fate of Internalized Virus.** HeLa cells were pretreated for 1 h with P16/16 or left untreated, and then mock-infected or infected at an MOI of 50 with HPV16 PsV containing FLAG-tagged L2. At 8, 16, and 24 h.p.i., cells were fixed, permeabilized, stained with antibody recognizing HPV16 L1, FLAG epitope, or LAMP1, and imaged. To detect L1 and L2 by immunoblotting, cells were infected as above at an MOI of 20. Extracts were prepared at 8, 16, and 24 h.p.i. After SDS/PAGE, samples were probed with antibodies recognizing L1, FLAG, and GADPH. In some experiments, cells were continuously treated with 100 μM CQ beginning 30 min prior to infection.

**Analyzing EdU-Labeled HPV16 Pseudovirus.** HeLa cells were infected at an MOI of 50 with HPV16 pseudovirus encapsidating EdU-labeled reporter plasmid. At a varying h.p.i., the cells were permeabilized, sequentially incubated with the Click-iT reaction mixture and antibodies recognizing cellular proteins, and processed for imaging.

**DMT1-II Localization.** HeLa-M cells (obtained from Walther Mothes, Yale University) were transfected with a plasmid expressing a GFP-tagged DMT1-II fusion protein (17). Six hours later, cells were treated with vehicle, 14 μM P16/16, or PDM/16. Eighteen hours after treatment, medium was replaced with fresh medium containing the same peptide concentration. Three hours later, cells were fixed, permeabilized, stained with anti-TGN46 or anti-EEA1 antibody, and imaged by confocal microscopy.

**Mouse Infection Experiments.** HPV16:pCLucF PsV was used to infect mice as previously described (18). Briefly, female FVB mice were injected subcutaneously with 3 mg medroxyprogestrone acetate. Five days later, anesthetized mice were treated intravaginally with 50 μL Conceptrol, which contains nonoxynol-9. Six hours later, anesthetized mice were mock-infected or infected intravaginally with HPV16:pCLucF PsV suspended in 4% carboxyl methyl cellulose. Some mice also received 25 μg P16/16 or PDM/16 in the viral inoculum. At 48 h.p.i., mouse female reproductive tracts were harvested and successful infection was assayed using an in vitro luciferase assay.

**Data Availability.** All data are available in the main text or the *SI Appendix*.

**ACKNOWLEDGMENTS.** We thank Christopher Burd, Craig Meyers, Christopher Buck, Catherine Deatherage, Walther Mothes, Akiko Iwasaki, John Schiller, Mac Crite, Patrick Buckley, and Mitsuaki Tabuchi for reagents and helpful comments. R.M. was supported by a training grant from the National Institute of Allergy and Infectious Diseases (T32 AI1078985). This work was supported by grants from the National Cancer Institute to P.F.L. (P01 CA022443, R35 CA210807) and by a grant from the National Institutes of Health to D.D. (R01 AI102876 and R01 CA037157).

1. C. B. Buck *et al*., Arrangement of L2 within the papillomavirus capsid. *J. Virol.* **82**, 5190–5197 (2008).
2. S. K. Campos, Subcellular trafficking of the papillomavirus genome during initial infection: The remarkable abilities of minor capsid protein L2. *Viruses* **9**, E370 (2017).
3. P. Zhang, G. Monteiro da Silva, C. Deatherage, C. Burd, D. DiMaio, Cell-penetrating peptide mediates intracellular membrane passage of human papillomavirus L2 protein to trigger retrograde trafficking. *Cell* **174**, 1465–1476.e13 (2018).
4. C. Burd, P. J. Cullen, Retromer: A master conductor of endosome sorting. *Cold Spring Harb. Perspect. Biol.* **6**, a016774 (2014).
5. P. M. Day, C. D. Thompson, R. M. Schowalter, D. R. Lowy, J. T. Schiller, Identification of a role for the trans-Golgi network in human papillomavirus 16 pseudovirus infection. *J. Virol.* **87**, 3862–3870 (2013).
6. A. Lipovsky *et al*., Genome-wide siRNA screen identifies the retromer as a cellular entry factor for human papillomavirus. *Proc. Natl. Acad. Sci. U.S.A.* **110**, 7452–7457 (2013).
7. A. Popa *et al*., Direct binding of retromer to human papillomavirus type 16 minor capsid protein L2 mediates endosome exit during viral infection. *PLoS Pathog.* **11**, e1004699 (2015).
8. W. Zhang, T. Kazakov, A. Popa, D. DiMaio, Vesicular trafficking of incoming human papillomavirus 16 to the Golgi apparatus and endoplasmic reticulum requires γ-secretase activity. *MBio* **5**, e01777-14 (2014).

9. C. B. Buck, D. V. Pastrana, D. R. Lowy, J. T. Schiller, Generation of HPV pseudovirions using transfection and their use in neutralization assays. *Methods Mol. Med.* **119**, 445–462 (2005).
10. A. Lipovsky, W. Zhang, A. Iwasaki, D. DiMaio, Application of the proximity-dependent assay and fluorescence imaging approaches to study viral entry pathways. *Methods Mol. Biol.* **1270**, 437–451 (2015).
11. E. Vives, C. Granier, P. Prevot, B. Lebleu, Structure-activity relationship study of the plasma membrane translocating potential of a short peptide from HIV-1 Tat protein. *Lett. Pept. Sci.* **4**, 429–436 (1997).
12. S. Fredriksson *et al*., Protein detection using proximity-dependent DNA ligation assays. *Nat. Biotechnol.* **20**, 473–477 (2002).
13. P. M. Day, C. C. Baker, D. R. Lowy, J. T. Schiller, Establishment of papillomavirus infection is enhanced by promyelocytic leukemia protein (PML) expression. *Proc. Natl. Acad. Sci. U.S.A.* **101**, 14252–14257 (2004).
14. P. M. Day *et al*., Human papillomavirus type 16 (HPV16) capsids mediate nuclear entry during infection. *J. Virol.* **93**, e00454-19 (2019).
15. S. DiGiuseppe, M. Bienkowska-Haba, L. G. M. Guion, T. R. Keiffer, M. Sapp, Human papillomavirus major capsid protein L1 remains associated with the incoming viral genome throughout the entry process. *J. Virol.* **91**, e00537-17 (2017).
16. M. Lucas *et al*., Structural mechanism for cargo recognition by the retromer complex. *Cell* **167**, 1623–1635 e14 (2016).
17. M. Tabuchi, I. Yanatori, Y. Kawai, F. Kishi, Retromer-mediated direct sorting is required for proper endosomal recycling of the mammalian iron transporter DMT1. *J. Cell Sci.* **123**, 756–766 (2010).
18. H. S. Huang, P. F. Lambert, Use of an in vivo animal model for assessing the role of integrin $\alpha(6)\beta(4)$ and syndecan-1 in early steps in papillomavirus infection. *Virology* **433**, 395–400 (2012).
19. G. Guidotti, L. Brambilla, D. Rossi, Cell-penetrating peptides: From basic research to clinics. *Trends Pharmacol. Sci.* **38**, 406–424 (2017).
20. Y. Cui *et al*., Retromer has a selective function in cargo sorting via endosome transport carriers. *J. Cell Biol.* **218**, 615–631 (2019).
21. A. Jimenez-Orgaz *et al*., Control of RAB7 activity and localization through the retromer-TBC1D5 complex enables RAB7-dependent mitophagy. *EMBO J.* **37**, 235–254 (2018).
22. S. Bhowmick, C. Chakravarty, S. Sellathamby, S. K. Lal, The influenza A virus matrix protein 2 undergoes retrograde transport from the endoplasmic reticulum into the cytoplasm and bypasses cytoplasmic proteasomal degradation. *Arch. Virol.* **162**, 919–929 (2017).
23. C. Elwell, J. Engel, Emerging role of retromer in modulating pathogen growth. *Trends Microbiol.* **26**, 769–780 (2018).
24. E. Groppelli, A. C. Len, L. A. Granger, C. Jolly, Retromer regulates HIV-1 envelope glycoprotein trafficking and incorporation into virions. *PLoS Pathog.* **10**, e1004518 (2014).
25. P. Yin, Z. Hong, X. Yang, R. T. Chung, L. Zhang, A role for retromer in hepatitis C virus replication. *Cell. Mol. Life Sci.* **73**, 869–881 (2016).
26. K. Harrison *et al*., Vaccinia virus uses retromer-independent cellular retrograde transport pathways to facilitate the wrapping of intracellular mature virions during virus morphogenesis. *J. Virol.* **90**, 10120–10132 (2016).
27. J. C. Hsiao *et al*., Intracellular transport of vaccinia virus in HeLa cells requires WASH-VPEF/FAM21-Retromer complexes and recycling molecules Rab11 and Rab22. *J. Virol.* **89**, 8365–8382 (2015).
28. S. Pillay *et al*., An essential receptor for adeno-associated virus infection. *Nature* **530**, 108–112 (2016).
29. H. Yan *et al*., Efficient inhibition of human papillomavirus infection by L2 minor capsid-derived lipopeptide. *MBio* **10**, e01834-19 (2019).
30. J. C. Jakobsen, E. E. Nielsen, R. L. Koretz, C. Gluud, Do direct acting antivirals cure chronic hepatitis C? *BMJ* **361**, k1382 (2018).
31. L. H. Pinto, R. A. Lamb, Understanding the mechanism of action of the anti-influenza virus drug amantadine. *Trends Microbiol.* **3**, 271 (1995).
32. J. C. Tilton, R. W. Doms, Entry inhibitors in the treatment of HIV-1 infection. *Antiviral Res.* **85**, 91–100 (2010).
33. S. Shi *et al*., Development of peptide inhibitors of HIV transmission. *Bioact. Mater.* **1**, 109–121 (2016).
34. Y. Luo *et al*., Interaction between simian virus 40 major capsid protein VP1 and cell surface ganglioside GM1 triggers vacuole formation. *MBio* **7**, e00297 (2016).